Int J Adv Manuf Technol (2015) 80:495–506
DOI 10.1007/s00170-015-7030-5

ORIGINAL ARTICLE

Numerical simulation of extrusion process and die structure optimization for a complex magnesium doorframe

Y. D. Sun [1] · Q. R. Chen [1] · W. J. Sun [1]

Received: 9 September 2014 / Accepted: 13 March 2015 / Published online: 28 March 2015

Abstract The numerical simulation of extrusion process for complex hollow magnesium doorframe is carried out using HyperXtrude software. According to the simulation results, the extrusion die structure has been optimized in this article. The flow velocity, welding pressure, and temperature distributions, as well as the particle tracking function provided by HyperXtrude are all adopted to affirm the structural rationality of the optimal die design schemes. The simulation results show that there is a great difference in metal flow velocity at the cross-section of extrudates for the initial die structure which is not suitable for production. The introduction of baffle plates in the lower die has balanced the metal flow to be more even through increasing the metal flow resistance in the parts where the flowing velocity is faster than in other parts. In the meanwhile, the optimal die structure with proper baffle plates exhibits higher welding pressure and more uniform temperature distribution in the extrudates. This could further improve the welding quality and eliminate the thermal deformation of the final profiles. According to the optimum die design scheme, the real mold has been manufactured and extrusion experiment has been carried out. The actual products exhibit favorable surface quality without twist deformation and dimension mistakes. Moreover, there is visible grain refinement in the microstructure of the extrudates. It has been proved that the die structure design based on the numerical simulation on the extrusion process with HyperXtrude could provide guidelines for complex hollow magnesium profiles and accelerate the production efficiency.

Keywords Magnesium profile extrusion · Baffle plate · Structure optimization · HyperXtrude

✉ Y. D. Sun
yingdisun@mail.sim.ac.cn

[1] Center of Advanced Magnesium Alloy and Protection, Shanghai Institute of Microsystem and Information Technology, Chinese Academy of Sciences, No. 865 Changning Street, Shanghai 200050, China

1 Introduction

As the lightest alloy in the structural materials, magnesium alloys have been widely used in the fields of automobile, aerospace, building, and information industries due to their low density, excellent bio-compatibility, superior specific stiffness, and strength [1–3]. At present, casting and plastic deformation are the primary forming methods for the application of magnesium alloys, while the mechanical properties of the latter are obviously better than those of the former because of the absence of casting defects and remarkable grain refinement for wrought magnesium alloys [4]. However, up till now, the wrought magnesium alloys have been found rather limited applications due to its hexagonal close-packed crystal structure and low deformability at temperatures below 225 °C [5, 6]. Accordingly, the fundamental understanding of the behavior of wrought magnesium alloys under hot deformation is of increasing significance, in which, hot-extrusion technology, as the typical forming process of magnesium alloys, has become the attentive focus in modern industry field.

The extrusion technology of magnesium alloys has attracted much attention in recent years because of its ability to achieve the superior precision, improved quality, and homogeneous properties throughout the component of the profile. Not only the solid and semi-solid profiles, but also the hollow magnesium profiles are manufactured through extrusion technology [7–9]. However, the preceding research has been primarily directed toward the simple solid profiles, such as magnesium bars and strips [8, 9]. Little study has been focused on the extrusion process of complex hollow ones due to the complex metal flow and welding process in the porthole die. Moreover, the postponed term and higher cost of testing die have still been the core difficult problems for the extrusion porthole die of hollow profiles. The complex structure of porthole die and the limited understanding of the metal flow in die cavity both impose resistance to the actual production. In general, the traditional design of extrusion dies is based on the trial-and-error method, and the performance of the dies is mainly dependent on the experience of die designers. Consequently, the product quality and productivity could not be guaranteed under this kind of design pattern.

With the development of computer technology, a great number of studies on the numerical simulation of extrusion process have been carried out to improve the product quality and production efficiency [10–12]. According to the numerical models, it is possible to predict flow velocities, temperature distributions, stress and strain gradients of the deforming metal, etc. Consequently, the optimum extrusion die structure and process parameters could be achieved and the defects twist, wave, bend, and crack could even be controlled. Currently, commercial software Deform-3D, Msc-SuperForge,

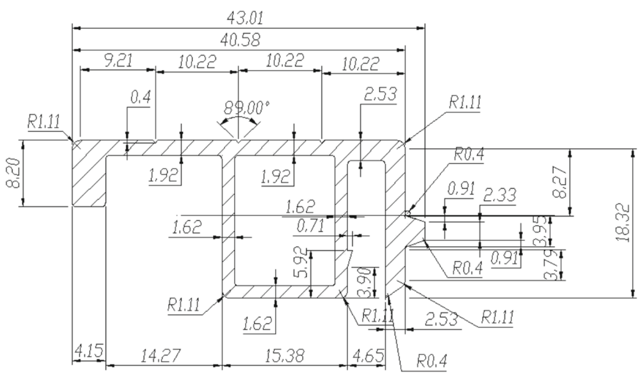

(a) 2D geometry and dimensions of the profile

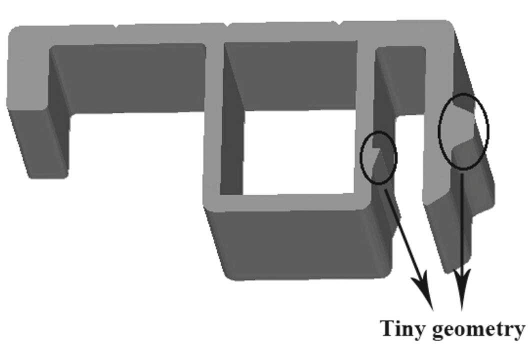

(b) 3D model profile

Fig. 1 Geometry and main dimensions of the hollow magnesium alloy profile studied in this work: **a** 2D geometry and dimensions of the profile; **b** 3D model profile

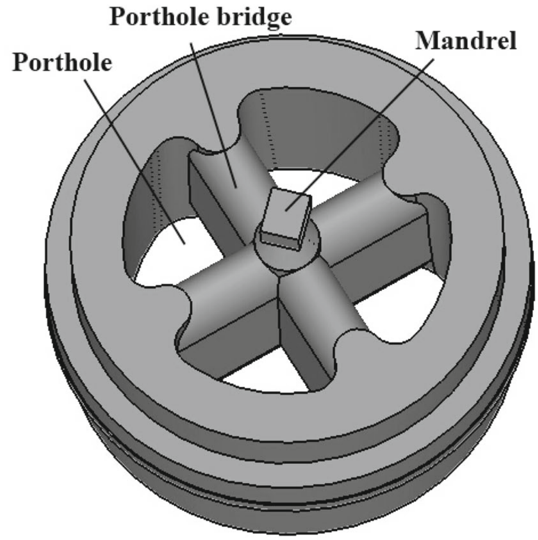

(a) Upper die

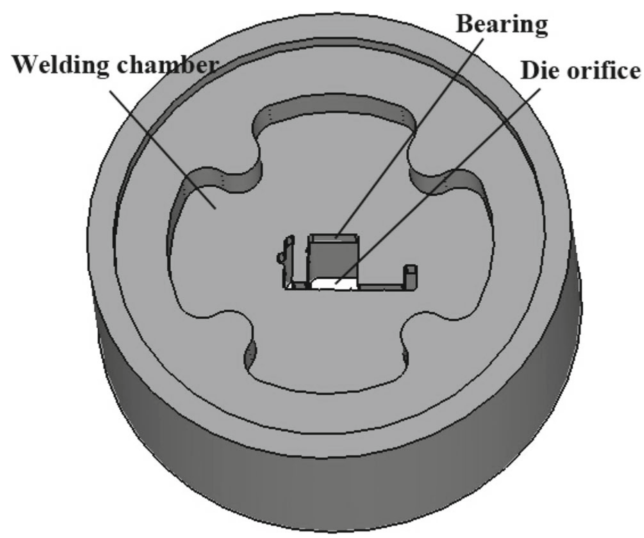

(b) Lower die

Fig. 2 3D model of the initial extrusion die structure: **a** upper die; **b** lower die

Fluent and HyperXtrude are being used for hot-extrusion die design extensively, in which, the Arbitrary Lagrangian Eulerian (ALE) program HyperXtrude is the first hp-adaptive finite element program [13]. HyperXtrude software alleviates many of the drawbacks that the traditional Lagrangian- and Eulerian-based finite element simulations have, and can be used to perform comprehensive engineering simulations, saving design and analysis engineer's time from performing several mesh generation and analysis cycles that are common with conventional [14]. In recent years, the application of HyperXtrude software has been used even more extensively. Bastani and co-workers have performed a

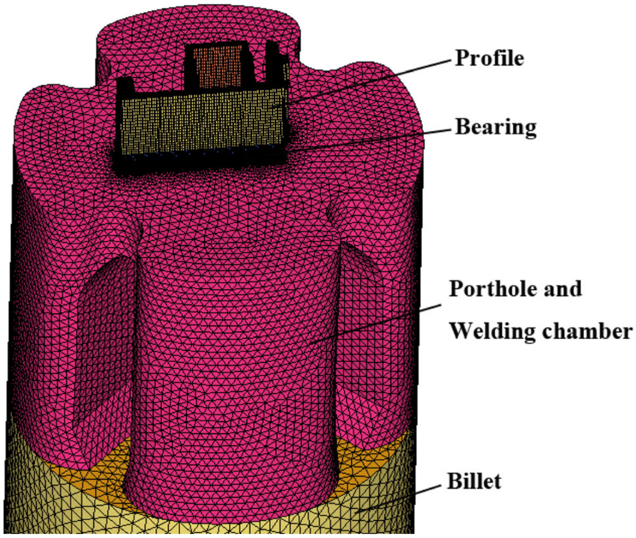

Fig. 3 The numerical simulation model of the extrusion process

transient simulation of the aluminum extrusion process based on ALE software HyperXtrude to find out how process parameters influence the flow balance and exit temperature [15]. Xu et al. have simulated the extrusion process of an aluminum multicavity wallboard profile using the ALE algorithm based HyperXtrude software and proposed three steps of the die optimization for the multicavity. The results show that the die optimization method based on numerical simulation is valid and can provide guidelines for die design. [16]. Zhang et al. has analyzed the metal flow behavior of an aluminum profile at each stage during the whole extrusion process and the dead zones in the die cavity based on the HyperXtrude, the numerical results are finally validated by comparing with the nose ends of two extrudates in practice [17]. Guan et al. have analyzed the design of a multihole extrusion die for producing an aluminum tube based on the results of metal flow, temperature distribution, welding pressure, extrusion load, and die stress which have been simulated and compared by means of HyperXtrude [18].

As can be seen from the previous research, a large number of studies by mean of HyperXtrude have been focused on the numerical simulation of extrusion process of aluminum alloys, while rare study could be found on the magnesium alloys, especially the complex hollow profiles. In this paper, the ALE method HyperXtrude has been adopted to model the extrusion process of a complex hollow magnesium profile. The material properties, mesh generation, boundary condition and process parameters will be described in detail. According to the numerical model, the flow behavior of magnesium alloys and deformation mechanism in the die cavity will be investigated with the analysis of velocity relative difference (VRD) of the extrudate. Then, the optimal die design schemes will be proposed and validated by the final practical extrudates. Moreover, the temperature distribution in cross-section of the extrudate, the welding pressure and velocity distribution in the welding chamber, as well as the metal flow pattern using the particle tracking function for the initial and optimal die design schemes will be analyzed and compared in this work.

2 Numerical simulation models with HyperXtrude

2.1 The initial die structure and geometry

Figure 1 shows the main dimensions and geometry of cross-section and 3D model of the hollow product in the present study. The profile exhibits its complexity of one center square cavity and two angle structures on both sides, as well as some tiny geometry features which are shown in Fig. 1b. The great difference in wall thickness of the profile, with the maximum and minimum wall thicknesses of 4.15 and 1.62 mm, determines its difficulty to control the metal flow uniformity during the extrusion process. Additionally, the section area of the

Table 1 Physical properties of AZ31 and H13

Material	Density/(kg m^{-3})	Specific heat/ [J(kg K)$^{-1}$]	Thermal conductivity/ [W(m K)$^{-1}$]	Thermal diffusion coefficient/K^{-1}	Young's modulus/Pa	Poisson's ratio
AZ31	1780	1200	96	2.2E−5	2.3E+10	0.35
H13	7870	548	28	1.3E−5	2.1E+11	0.35

Table 2 Process parameters applied in simulation

Billet diameter/mm	Billet length/mm	Initial temperature of billet/K	Initial temperature of die/K	Initial temperature of container/K	Ram speed/(mm s^{-1})	Extrusion ratio
90	400	420	480	450	1	23

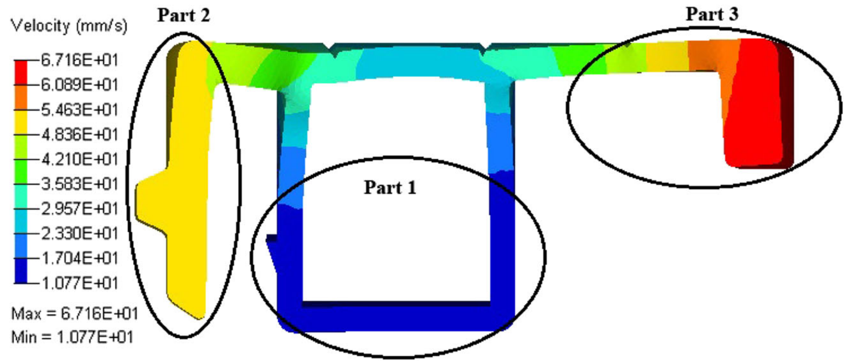

Fig. 4 The velocity distribution at the cross-section of the extrudate with the initial die structure scheme

profile is 215.4 mm^2. Considering its complex structure and extruded product quality, the split ratio should be increased properly, about 20~30, this determines the total area of the portholes in some degree. Above all, to balance the metal flow and gain the qualified products, more attention should still be paid on the design of die structures.

In the present work, the flat porthole die is chosen for the production of magnesium hollow profile. Figure 2 shows the 3D model of the initial die structure, including the upper and lower dies, as shown in Fig. 2a, b, respectively. The upper die is mainly composed of four parts: porthole, port bridge, and mandrel, as well as drainage channel only for multicavity profile. The portholes are designed to split the metal flow around the mandrel to form the hollow extrudate. The port bridge is the connection of portholes, supporting the die mandrel. The die mandrels are mainly designed to form the inner contour of hollow cavity in the profile. The drainage channel is generally designed between the mandrels to accelerate the metal flow through the wall of multiholes profile. In this work, four portholes and water-type port bridge are designed in the upper die in order to allocate and weld material rationally. Due to the single-hole structure of the profile in this case, there is no design of the drainage channel. According to the area of the profile, the final split ratio is approximately 23. Meanwhile, the outer diameter and height of upper die are 149 and 66.5 mm, respectively. The lower die with responsibility for the formation of final product is mainly composed of three parts: welding chamber, bearing and die orifice, as shown in Fig. 2b. The welding chamber takes charge in the joining of the metal flowing from the portholes, and then pushing the metal accumulated in the chamber through the die orifice. The bearing bands appearing in the mandrels of upper die and orifice of lower die are mostly used to control the metal flow and surface quality of the final profiles. In this case, the outer diameter and the height of the lower die are 149 and 57 mm, respectively. The initial height of the welding chamber is 14 mm.

2.2 Mesh generation of simulation model

Before the numerical simulation of extrusion process by means of HyperXtrude, it is necessary to extract and mesh

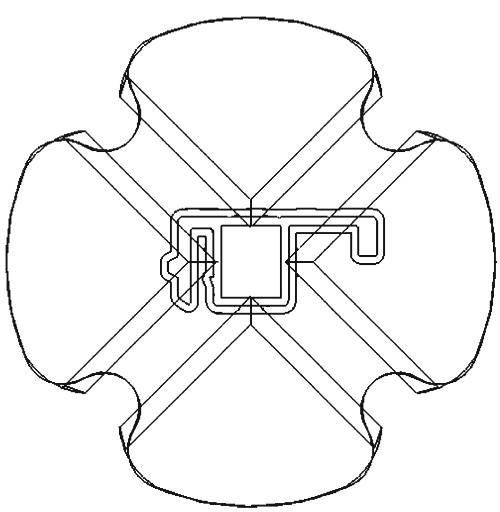

Fig. 5 The position relation between the portholes and extrudate for the initial die design

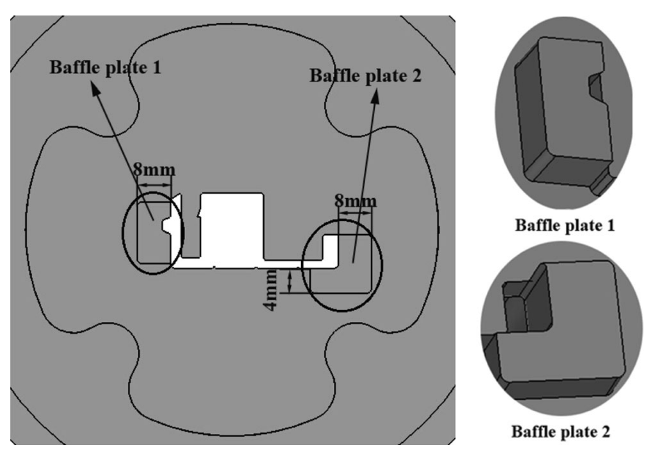

Fig. 6 The structure modification of the first optimal die design scheme

all fields material flows through. The first step is to import the 3D geometries of the extrusion dies into Hypermesh, and then manually delete untrimmed surfaces, set the cleanup tolerance and correct any errors in the geometries from import. Lately, the simplified parts needed for the analysis are created, including billet, portholes, weld chamber, bearing, and so on. Considering the control of element number and calculation accuracy, it is necessary to assign different element types and sizes at different parts of the numerical model. This is also consistent with the extent of local deformation. The meshing option starts with the bearing region which often undergoes severe shear deformation to form the final shape of the profile. Thus, finer triangular prism elements are adopted in the regions of bearing and profile, while setting a constant element length (usually four elements) in the flow direction. In the meanwhile, the relatively coarse tetrahedral elements are used in the regions of welding chamber, porthole, and billet with the minimum element of 0.2 mm. The element number of whole model is about 130,000. Figure 3 shows the simulation model for the metal flow analysis, including five parts: billet, porthole, welding chamber, bearing, and profile. In which, for simplicity, the porthole and welding chamber are combined together as one part for simulation.

2.3 Definition of material parameters

Arrhenius equations are often employed to mathematically determine flow stress as a function of parameters such as strain, strain rate, temperature, and so on, typically shown as the following [19]:

$$\dot{\varepsilon} = A[\sin(\alpha\sigma)^n[\exp(-Q/RT)]] \quad (1)$$

where $\dot{\varepsilon}$ is the effective strain rate, σ is the flow stress, n, A, and α are the temperature-independent material parameters, Q is the activation energy, T is the absolute temperature, R is the universal gas constant. According to our previous research, parameters values used for AZ31 in this work are as follows

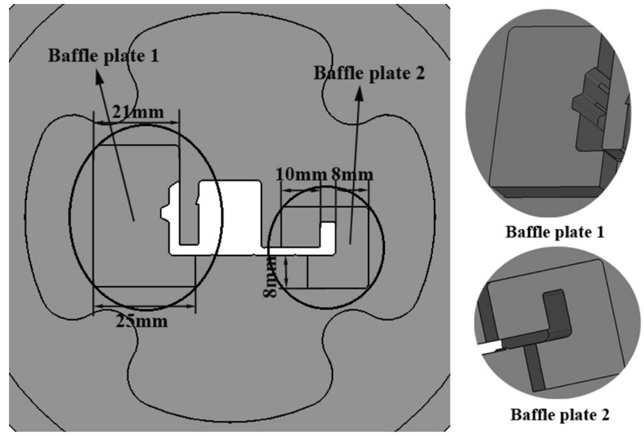

Fig. 8 The structure modification of the second optimal die design scheme

[20]: Q=218 kJ/mol, R=8.314 J/(mol K), A=2.8×10^{-16}, n=7.875, and α=0.014. In addition, H13 is chosen as the die material, the physical properties of AZ31 and H13 are given in Table 1.

2.4 Boundary conditions and process parameters

In the HyperXtrude software, ten kinds of boundary conditions have been offered to define the numerical model. In which five kinds of conditions are adopted in this work, including inflow-type (billet-dummyblock), solidwall-type (billet-container, billet-die, porthole-die), bearing-type (bearing-die), freesurface-type (freesurface), and outflow-type (exit). In the real extrusion process, the friction conditions of the boundaries play an important role in the quality of final profiles. Considering the adhesion extent and local deformation at different boundaries, the surfaces in contact with the bearings all adopt the slipping friction condition with a factor of 0.3, while the other interfaces between the billet and tooling use the fully sticky friction condition.

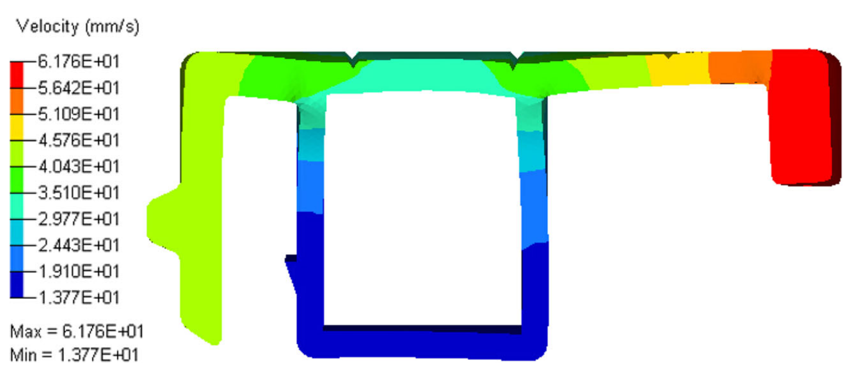

Fig. 7 The velocity distribution at the cross-section of the first optimal die design scheme

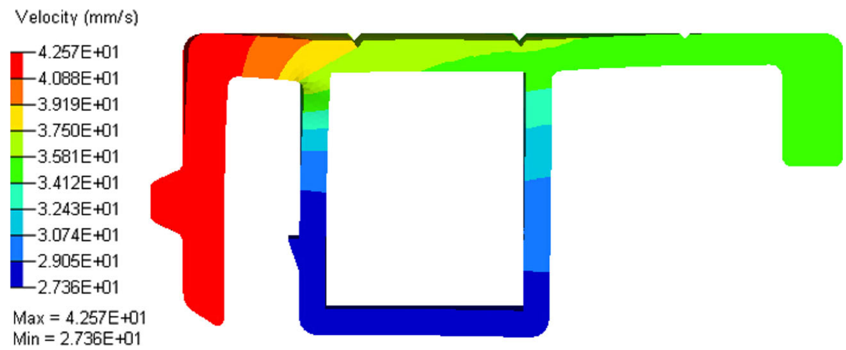

Fig. 9 The velocity distribution at the cross-section of the second optimal die design scheme

Moreover, the process parameters play the same important role as the boundary conditions in the extrusion process. The definition of the process parameters more depend on the experience of practical production. Table 2 gives the process parameters applied in the simulation, including the size of billet, initial temperature of billet and tool (die and container), ram speed, as well as extrusion ratio. The numerical simulation is performed in the workstation with CPU i7-4770 and 16G of RAM. The whole simulation needs about 10 h.

3 Numerical simulation results and discussion of the initial die structure

According to the numerical simulation of the initial die structure, a large number of results can be obtained, such as the distribution of velocities, strains, stresses, temperatures, and extrusion forces, etc,, in which the metal flow velocity over the cross-section of the profile exit is of great importance to judge the rationality of the die structure and the final profile quality. Figure 4 shows the velocity distribution at the cross-section of the extrudate obtained from the simulation. As can be seen from the figure, there is a great difference in metal flow velocity of the whole profile exit, which can be divided into three parts, as shown in Fig. 4 (part 1~part 3). Part 1 is mainly located in the square hole which exhibits the lowest velocity (17.04~29.57 mm/s) throughout the whole exit. In general, the metal velocity will always be restricted for the limited flowing space when metal flows through the hollow region, especially in this case with relatively thinner wall thickness. In contrast, the metal velocities of part 2 and part 3 are visibly larger than part 1, and the maximum velocity is obtained by part 3. This could be ascribed to the larger wall thicknesses in the two sides of the extrudate. Moreover, the position of portholes in the upper die plays a very effective role in balancing the metal flow. Figure 5 gives the structural distribution of the portholes for the initial die design. As can be seen, the three parts in the cross-section of the extrudate are located in different position of the portholes. For example, the whole part 1 is under the region of bridge, far away from the portholes, which determines the limited metal flow velocity. Parts 2 and 3 are both distributed under the portholes, implying that the material supply here for these parts is excessive. This renders a possible explanation for the faster flowing velocity of the part 2 and 3 in comparison to part 1. In order to make the flow velocity distribution of the exit more uniform, it is necessary to restrict the metal flow of part 2 and 3.

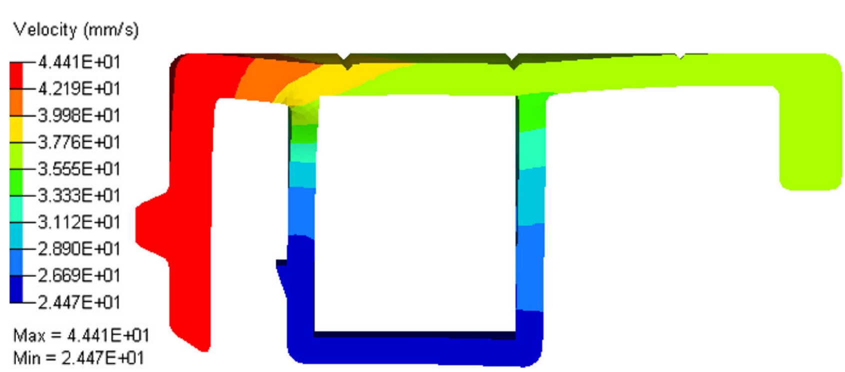

Fig. 10 The velocity distribution at the cross-section of the second optimal die design scheme with 5-mm-high baffle plates

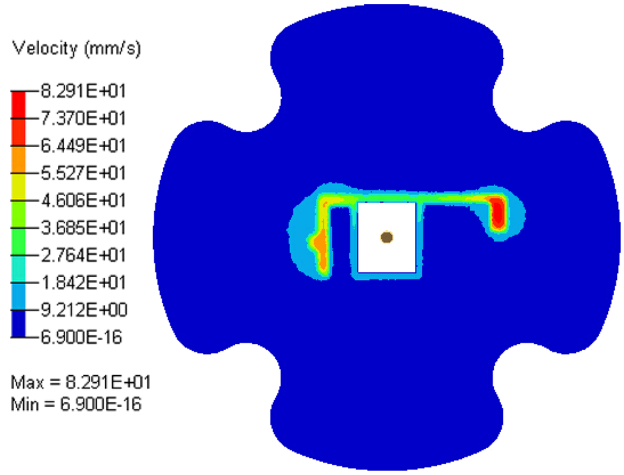

(a) The initial die design

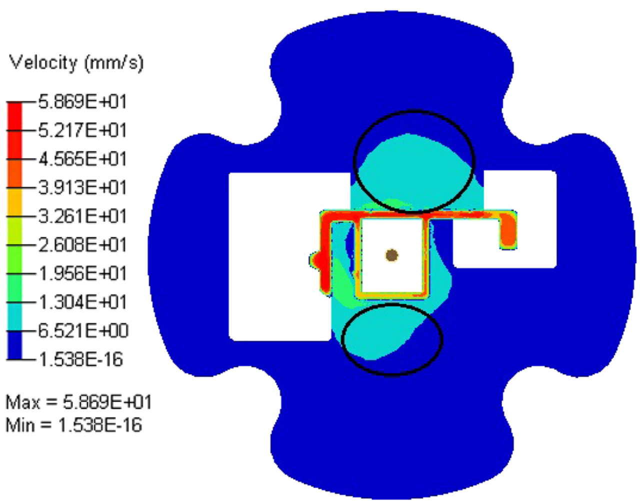

(b) The optimum die design

Fig. 11 Comparison of the metal flow at the inlet of the die orifice: **a** the initial die design; **b** the optimum die design

To judge the extent of metal velocity uniformity over the cross-section of the exit, the SDV parameter is introduced in this work, which can be expressed as [21]:

$$\mathrm{SDV} = \sqrt{\frac{\sum_{i=1}^{N}(v_i - v_{\mathrm{ave}})^2}{N}} \tag{2}$$

where v_i is the velocity at node i in the cross-section of the extrudate, v_{ave} is the average velocity of all nodes to be researched, N is the number of nodes. It has been confirmed that the smaller SDV values, the more uniform velocity distribution and the better the quality of extrudates. In this case, 50 nodes in the cross-section of extrudate have been chosen to calculate the SDV, and the final value of the initial die structure is 13.22. It is obvious that the initial die design scheme is not reasonable for the high SDV value, this will cause defects such as twist, bend, and dimensional error of the final profile. Therefore, it is necessary to do some modification of the die structure to balance the metal flow and further to improve the quality of extrudate. In this article, the optimization work will be carried out based on the design of the baffle plates in the lower die to reduce the velocity of part 2 and part 3.

4 Optimization of the die structure

To balance the metal flow velocity of the exit in the profile, the adjustments in the position and shapes of portholes as well as the bearing length are always introduced in the design of extrusion die. In this case, however, the efficiency of the above means is apparently decreased due to the structural characteristics of the profile. First of all, there is little effect of porthole sizes on the metal flow velocity of part 1 in the extrudate. Moreover, according to the previous experience of die design [22], the amendment of bearing length is relatively limited to improve the metal flow uniformity of the hollow and unsymmetrical extrudate. Therefore, in this article, the method of baffle plate has been proposed to control the metal flow in the cavity of the die.

The baffle plate is always designed closely with the bearing in the welding chamber and located in the place with lower flow resistance. In general, where the flow resistance is relatively small, a higher baffle plate in the welding chamber is designed to guide the metal to flow into the part which is difficult to form. Thereby, the velocity of metal flow of the final extrudate could be controlled to be uniform.

4.1 Simulation results and discussion of the first optimal die structure

According to the simulation results of the velocity distribution of initial die structure, it is necessary to promote the metal flow of part 1 and restrain the flow velocities of part 2 and 3 to make the flow uniformity. Therefore, baffle plates 1 and 2 are introduced in the first optimal die structure, as shown in Fig. 6. The basal dimensions of the baffle plates are labeled in the figure with 7 mm in height. The simulation results of velocity distribution of the first optimal die structure are shown in Fig. 7. Comparing with the results of initial die structure, the velocity difference of the first optimal scheme in the cross-section of the extrudate is partly reduced while the distribution of the velocity in the cross-section changes slightly. The maximum velocity is still received by part 3 (~61.76 mm/s) and the minimum velocity is distributed in part

Fig. 12 Comparison of the metal flow near the baffle plates with particle tracking: **a** the initial die design; **b** the optimum die design; **c** the longitudinal graph of metal flow streamlines for optimum die design

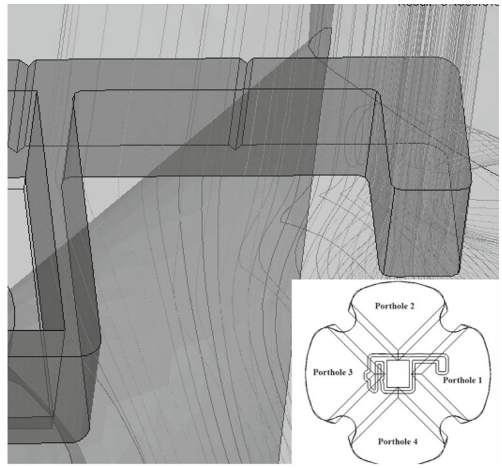

(a) The initial die design

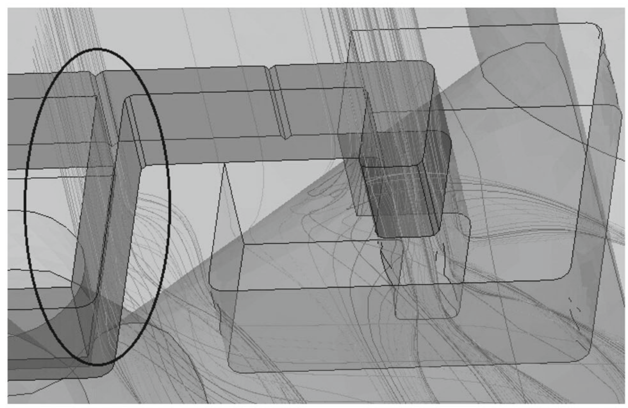

(b) The optimum die design

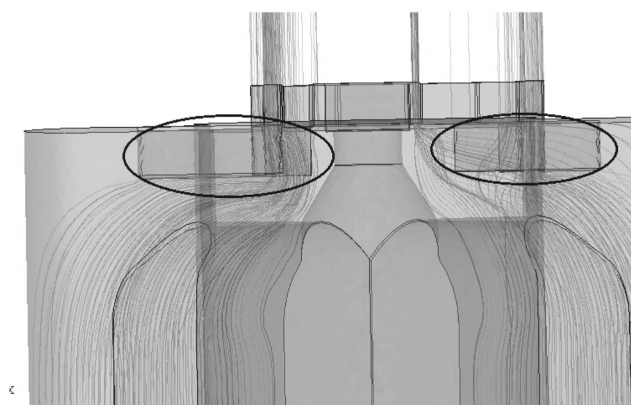

(c) The longitudinal graph of metal flow streamlines for optimum die design

1 (~13.77 mm/s). Through calculation, the SDV is reduced to 10.51, indicating that the introduction of baffle plate 1 and 2 indeed improve the uniformity of flowing velocity in the extrudate. However, the above improvement results have not satisfied the requirements of extrusion process.

4.2 Simulation results and discussion of the second optimal die structure

Based on the simulation results of first optimal die structure, the sizes of baffle plates 1 and 2 are apparently needed

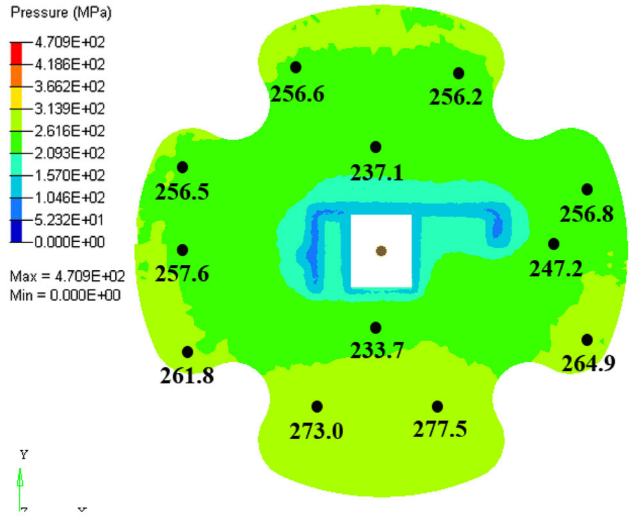

(a) The initial die design

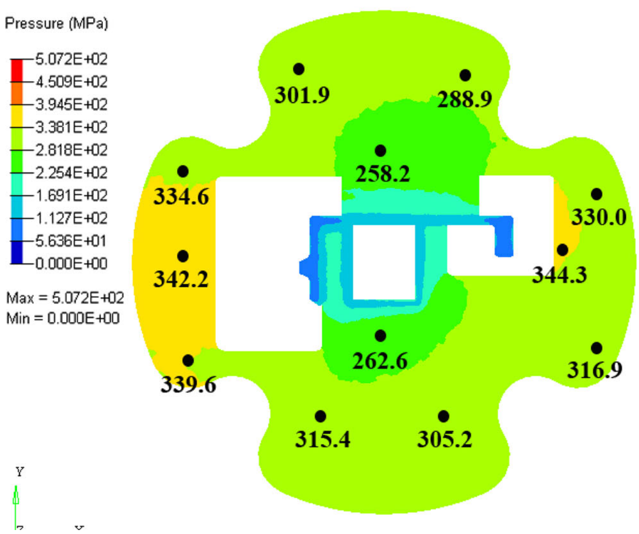

(b) The optimum die design

Fig. 13 Comparison of pressure distribution in the welding chamber: **a** the initial die design; **b** the optimum die design

to be increased properly to further slow down the metal flow in part 2 and 3 with the same height as first optimal die. The amendment details are shown in Fig. 8. According to the second optimal scheme, the extrusion process is simulated again with the identical process parameters to the previous simulation. The distribution of metal flow velocity is shown in Fig. 9. It can be observed that the velocity distribution in the second optimal scheme varied largely compared to the results of initial and first optimal numerical simulation, the velocity difference in the cross-section of the extrudate is greatly reduced (the velocity region is from 27.36 to 42.57 mm/s). The velocity distribution in the cross-section of the extrudate has even been changed apparently for the velocity of part 3 is markedly decreased from 61.76 to 35.81 mm/s, lower than that of the part 2. The corresponding SDV is reduced to 5.06, less than the half of initial one.

In order to identify the height effect of baffle plates on the metal flow distribution, the baffle plates 1 and 2 with height of 5 mm and same sizes in plane as the second optimal scheme are introduced in the further amending scheme, and the simulation results of velocity distribution in the cross-section of extrudate is shown in Fig. 10. As can be seen from this figure, the decreasing height of baffle plates does not change the distribution of the velocity in the cross-section comparing with the second die structure, but enlarge the region of velocity difference throughout the exit (24.47~44.41 mm/s). Furthermore, the SDV value increases to 6.39, which is obviously larger than that of the second optimal scheme. Thus, the second optimal die structure with 7-mm-height baffle plates is more rational and satisfactory to make the material supply more even in the cross-section of the extrudate, and could be put into the practical production.

4.3 Comparison and discussion of the initial and optimum die design schemes

Figure 11 gives the metal flow status at the inlet of the die orifice of initial and optimum die structures. In fact, before the materials encounters the baffle plate in the welding chamber, the metal flow status keeps almost invariant before and after the optimization of the die structure. From Fig. 11, it could be seen that the introduction of baffle plates 1 and 2 indeed increase the materials supply of part 1 (hollow part, as marked with a circle) and further promote the metal flow in this part. Accordingly, the flow velocities of part 2 and 3 are apparently decreased. The flow velocity streamlines (particle tracking function available in HyperView) could offer the more intuitionistic explanations for the metal flow characteristics of the optimal die structure with baffle plates, as shown in Fig. 12. In general, more metal streamlines exist, metal flows faster, and thus, the distribution of metal streamlines in the die cavity stands for the velocity value of metal flow. For the initial die structure, the materials flowing through the porthole 1 are mostly supplied for part 3 of the extrudate (as shown in Fig. 12a), while the existence of baffle plates guides part of the materials to flow away from the initial path but through the hollow section of part 1 (as marked in circle of Fig. 12b). Figure 12c is the longitudinal graph of flow velocity streamlines for the optimum die structure. As can be seen from this figure, when the metal flow encounters the baffle plates (as marked with circle in the two sides), the resistance of the metal flow will enhance, and

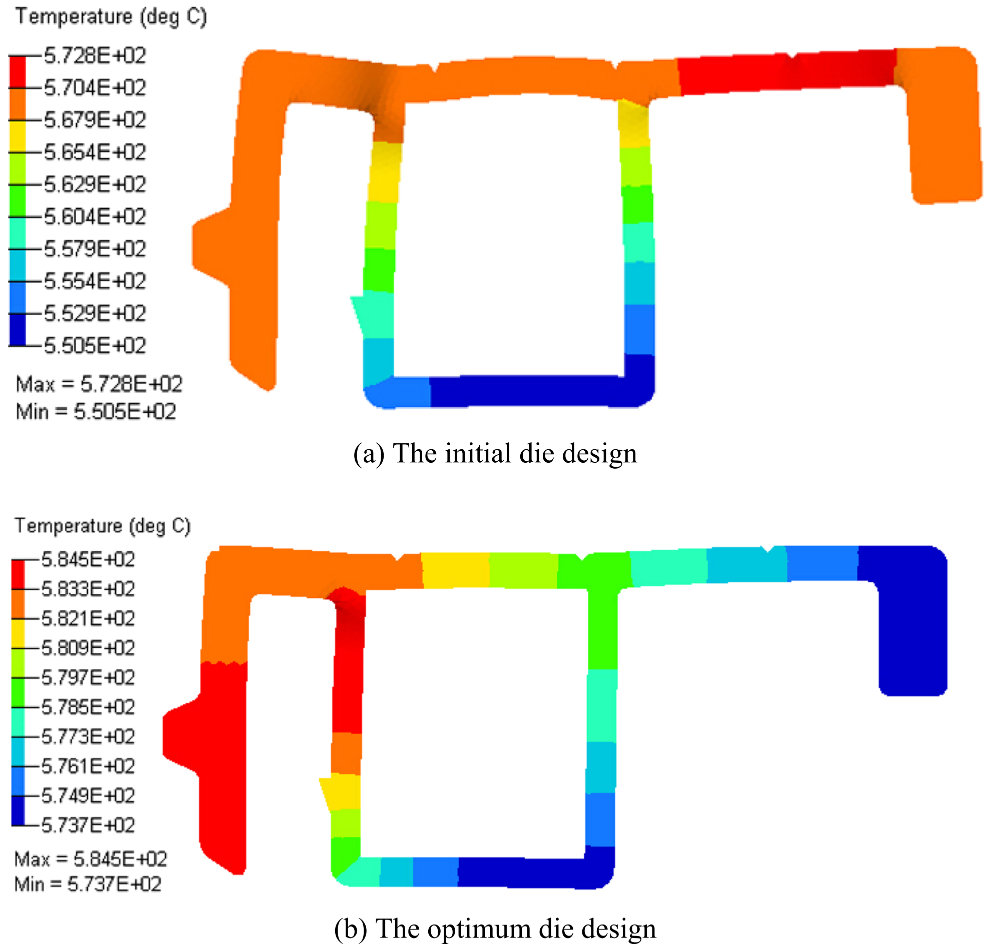

Fig. 14 Comparison of temperature distribution at the cross-section of the extrudate: **a** the initial die design; **b** the optimum die design

thus the materials will easily be pushed into the region that is difficult to form around the baffle plate and the metal flow could be balanced effectively.

The welding pressure distributions in the welding chamber of the initial and optimal die schemes are shown in Fig. 13. It could be found out that the pressure in the welding chamber after optimization is apparently larger than that of the initial one, the increase in amplitude is about 20 %. This could be ascribed to the introduction of the baffle plates which increase the friction of the metal flow near the die orifice. With the increase of welding pressure, the welding quality could be further improved and the extruding speed is able to accelerate accordingly.

Figure 14 gives the temperature distribution in the cross-section of the extrudate for the initial and optimal die schemes. According to the comparison of temperature region, it is clearly seen that the temperature distribution for the optimal die design is more uniform compared to that of the initial die design, for the temperature range is only 11 °C for the former die which is smaller than that of the later die (22 °C). This is because the optimal scheme with baffle plates could balance the metal flow effectively, and the plastic deformation heat is distributed more evenly. Due to the uniform distribution of temperature for the optimization scheme, the thermal deformation of the final profiles could be further eliminated.

5 Experiments and discussions

To validate the rationality of the optimal die structure in this work, the real mold is manufactured according to the optimum design scheme and the practical profile extrusion is carried out. The process parameters adopted in extrusion experiments were exactly the same as the numerical simulations. Figure 15a, b shows the photographs of the actual dies and profiles. As can be seen from the figures, the extruding profiles avoid the defects like twist deformation as well as general dimension errors, and exhibit the preferable surface quality. This is implying that the die design structure optimized in the numerical simulation is of great reference value and could provide useful guidelines for practical production. Figure 15) gives the optical micrographs of the microstructure of the

(a) The actual dies

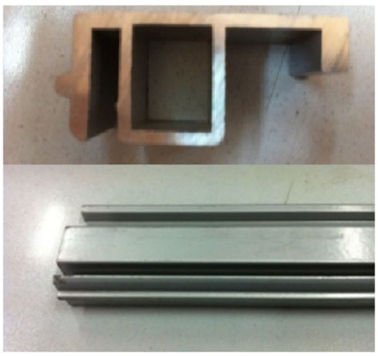

(b) The proile

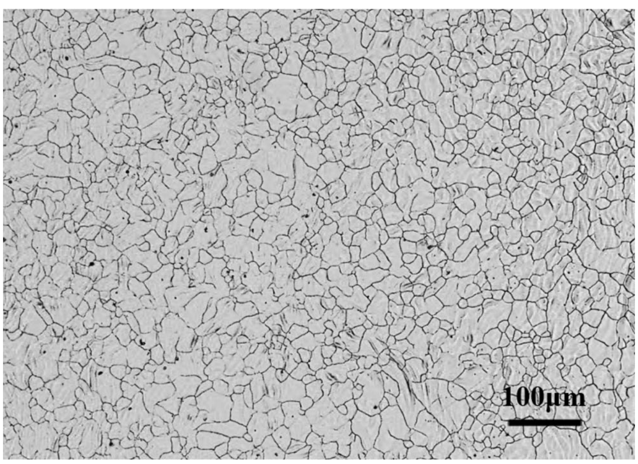

(c) Microstructure of the extrudates

Fig. 15 Photographs of the actual dies, profiles and microstructure of the extrudates: **a** the actual dies; **b** the profile; **c** microstructure of the extrudates

extrudates. It is clear that the grain is refining markedly and well distributed after extrusion.

6 Conclusions

In this article, the numerical simulation of extrusion process and the die structure optimization procedure for a complex hollow magnesium profile has been described in detail. The flow velocity, welding pressure and temperature distributions, as well as the particle tracking function provided by HyperXtrude are all introduced to analyze the extrusion process and structural rationality of the optimal die design schemes. The conclusions have been drawn as follows:

1. The baffle plate introduced in the lower die is of great importance in the balance of the metal flow. Through the restriction of the material flowing in the local regions with lower resistance, more material has been guided to flow into the part which is difficult to form.
2. The optimal die structure with proper baffle plates exhibits higher welding pressure and more uniform temperature distribution in the extrudates. This could be ascribed to the introduction of the baffle plates which not only increase the friction of the metal flow near the die orifice, but also balance the flowing velocity effectively.
3. The real mold has been manufactured according to the optimum scheme and the extrusion experiment has been carried out. The extruding products avoid the general defects like twist deformation and dimension errors, showing excellent surface quality. The microstructure of the extrudates exhibits the remarkable grain refinement.
4. The reasonable design of the baffle plates presented in this article based on the numerical simulation through HyperXtrude has been proved to be efficient for the optimization of complex die design and provided guidelines for the extrusion production of complex magnesium hollow profiles.

References

1. Yu X, Li YL, Li L (2014) Effect of grain refinement on fracture toughness and fracture mechanism in AZ31 magnesium alloy. Procedia Mater Sci 3:1780–1785
2. Torbati-Sarraf SA, Langdon TG (2014) Properties of a ZK60 magnesium alloy processed by high-pressure torsion. J Alloys Compd 613:357–363
3. Asgari H, Szpunar JA, Odeshi AG (2014) Texture evolution and dynamic mechanical behavior of cast AZ magnesium alloys under high strain rate compressive loading. Mater Des 61:26–34
4. Stráská J, Janeček M, Čížek J, Stráský J, Hadzima B (2014) Microstructure stability of ultra-fine grained magnesium alloy AZ31 processed by extrusion and equal channel angular pressing (EX-ECAP). Mater Charact 94:69–79
5. Mirzadeh H (2014) Constitutive analysis of Mg-Al-Zn magnesium alloys during hot deformation. Mech Mater 77:80–85
6. Dong HW, Pan FS, Jiang B, Zeng Y (2014) Evolution of microstructure and mechanical properties of a duplex Mg-Li alloy under extrusion with an increasing ratio. Mater Des 57:121–127

7. Zhang DQ, Chen GP (2012) The numerical simulation for extrusion forming of magnesium alloy pipes. Phys Procedia 25:125–129
8. Tong LB, Zheng MY, Cheng LR, Kamado S, Zhang HJ (2013) Effect of extrusion ratio on microstructure, texture and mechanical properties of indirectly extruded Mg-Zn-Ca alloy. Mater Sci Eng A 569:48–53
9. Yang QS, Jiang B, He JJ, Song B, Liu WJ, Dong HW, Pan FS (2014) Tailoring texture and refining grain of magnesium alloy by differential speed extrusion process. Mater Sci Eng A 612:187–191
10. Gamage P, Xie SQ (2009) A real-time vision system for defect inspection in cast extrusion manufacturing process. Int J Adv Manuf Technol 40:144–156
11. Bikass S, Andersson B, Pilipenko A, Langtangen HP (2012) Simulation of initial cooling rate effect on the extrudate distortion in the aluminum extrusion process. Appl Therm Eng 40:326–336
12. Malayappan S, Narayanasamy R (2004) An experimental analysis of upset forging of aluminium cylindrical billets considering the dissimilar frictional conditions at flat die surfaces. Int J Adv Manuf Technol 23:636–643
13. Mayavaram R, Sajja U, Secli C, Niranjan S (2013) Optimization of bearing lengths in aluminum extrusion dies. Procedia CIRP 12: 276–281
14. He Z, Wang HN, Wang MJ, Li GY (2012) Simulation of extrusion process of complicated aluminum profile and the die trial. Trans Nonferrous Metals Soc China 22:1732–1737
15. Kumar S, Vijay P (2007) Die design and experiments for shaped extrusion under cold and hot condition. J Mater Process Technol 190:375–381
16. Bastani AF, Aukrust T, Skauvik I (2010) Study of flow balance and temperature evolution over multiple aluminum extrusion press cycles with HyperXtrude 9.0. Key Eng Mater 424:257–264
17. Xu L, Zhao GQ, Zhang CS, Chen H, Li HK (2011) Numerical simulation of extrusion process and die optimization for aluminum multi-cavity profile. J Mech Eng 47:61–68
18. Zhang CS, Zhao GQ, Chen H, Guan YJ, Kou FJ (2012) Numerical simulation and metal flow analysis of hot extrusion process for a complex hollow aluminum profile. Int J Adv Manuf Technol 60: 101–110
19. Guan YJ, Zhang CS, Zhao GQ, Sun XM, Li P (2012) Design of a multihole porthole die for aluminum tube extrusion. Mater Manuf Process 27:147–153
20. Sellars CM, Mctegart WJ (1966) On the mechanism of hot deformation. Acta Metall 14:1136–1138
21. Li GZ, Sun YD, Chen QR, Zhang Y (2015) Numerical simulation of extrusion process and die structure optimization for the magnesium profile based on HyperXtrude. Hot Working Technology, accepted
22. Halvorsen F, Aukrust T (2006) Studies of the mechanisms for buckling and waving in aluminum extrusion by use of a lagrangian FEM software. Int J Plast 22:158–173